Output-Feedback Control of the Longitudinal Flight Dynamics Using Adaptative Backstepping

F. Gavilan, R. Vazquez and J.Á. Acosta

Abstract— **An adaptive backstepping approach is used to design an output feedback control law for the longitudinal dynamics of an Unmanned Air Vehicle (UAV). The resulting nonlinear controller makes the system follow references in the aerodynamic velocity and flight path angle, using elevator deflections and thrust as actuators. Only measurable quantities are used in the control and adaptation laws. The proposed strategy allows to design an explicit controller without any knowledge of the aerodynamic coefficients or the trim angle of attack, which also depends on the the aerodynamic coefficients; only well-known qualitative physical properties from aerodynamics are used. Simulations are included for a realistic UAV model that includes actuator saturation.**

I. Introduction

In recent years, the interest in unmanned air vehicles (UAVs) has increased considerably. Not having a pilot makes aircraft lighter, cheaper and more efficient for missions such as surveillance or reconnaissance. The absence of a pilot implies that the design of an adequate automatic flight control system has a crucial role in the UAV design process.

The main difficulty in the design of an automatic flight control system is the absence of effective mathematical models valid for all flight conditions. Aerodynamic forces and moments appearing in the flight mechanics equations are not only highly nonlinear, but also very difficult to model accurately.

Traditionally, flight controllers have been designed based on a linearized aircraft model for a selected operating point. Using the linear model, a range of control techniques can be then applied [1]. However, when the flight condition is changed, the model is no longer valid and the controller performance can be compromised. To overcome this difficulty, gain scheduling methods have been applied in the past [2]. However, these methods have the need of computing different controllers for different operating points and estimating aircraft stability derivatives for a wide range of flight conditions, which can be a very cumbersome task.

Nonlinear control methods are natural candidates to deal with these difficulties. For instance, feedback linearization [3] has been proposed to generate feedback laws suitable for all the flight envelope, if a precise model of the aircraft is known; however, this is not usually the case. Backstepping is another nonlinear control technique which can handle nonlinearities, for systems with a cascade structure [4]. For systems with parametric uncertainties, the *adaptive backstepping* control technique can guarantee system stability without exact knowledge of the model. This makes adaptive backstepping a very useful tool for flight control system design, given the fact that accurate aerodynamic and propulsive models are seldom available.

Several examples of backstepping applied to flight control can be found in the literature. For instance, [5] develops some aircraft flight controllers which use this technique; the aerodynamic moments are used as virtual control signals in the backstepping design, and a control allocation scheme is used to find the aerodynamic surface deflections.

In [6] an adaptive backstepping flight controller for a high-performance UAV is developed, guaranteeing Lyapunov stability and including physical constraints in the control system, such as saturations, bandwidth limitations or rate limits. A linear aerodynamic model is used, with adaptation laws to estimate online the stability derivatives in the model. A similar approach is described in [7], where a constrained adaptive backstepping controller is designed for the F-16/MATV simulation model, representing its aerodynamics with neural networks whose weights are estimated through adaptation laws.

The objective of this paper is to develop an output-state feedback law for aircraft longitudinal dynamics that works for all the normal operating regimes of the aircraft, and needs *minimal* information of the aerodynamic model. The control objective is to seek references in the aerodynamic velocity and flight path angle, using as actuators the elevator deflections and the thrust level. An adaptive backstepping strategy is proposed, which exploits the structure of the system and well-known *qualitative* properties from aerodynamics. The nonlinear longitudinal aircraft model is used, and, since only some specific properties of the aerodynamic coefficients are known, an adaptation law is designed for their online estimation. The controller for velocity and flight path angle are designed separately. The resulting control laws are explicit and simpler than those produced by the previously cited works, and do not require much computational power on board. Simulations are included for a realistic UAV model that includes actuator saturation and nonlinear dynamics. The model is a description of the Cefiro aircraft [8], an UAV recently designed and constructed in the University of Seville.

F. Gavilan and R. Vazquez are with the Department of Aerospace Engineering, Universidad de Sevilla, Camino de los Descubrimientos s.n., 41092 Sevilla, Spain. (e-mails: fgavilan,rvazquez1@us.es).

J.Á. Acosta is with the Depto. de Ingeniería de Sistemas y Automática, Universidad de Sevilla, Camino de los Descubrimientos s.n., 41092 Sevilla, Spain. (e-mail: jaar@us.es).

Contribution. The basis of this work is our previous full-state feedback design presented in [9]. In that work, we were able to solve the problem but assumed some knowledge of aircraft aerodynamics. In particular, we made use of the trim angle of attack (which depends on the desired reference and the aerodynamics coefficients) and the coefficient $C_{m_{\delta_e}}$ (which multiplies the elevator deflection actuation). In this paper we drop both hypothesis, using only physically measurable quantities and estimating all the coefficients. Thus, the controller is formulated without using any aerodynamics model; only fundamental properties of aerodynamics (which are true for all aircraft) are used in the design.

The paper is structured as follows: First, in Section II aircraft model used in this work is presented. The controller design is detailed in Section III, which begins with the velocity controller (III-A) and follows with the flight path angle controller (III-B). Simulation results are shown in Section IV. Section V closes the paper with some concluding remarks.

II. AIRCRAFT LONGITUDINAL FLIGHT MODEL

Let $(V_a, \gamma, \theta, q) \in \mathbb{R}^4$ be the state vector where V_a is the aerodynamic velocity, γ is the flight path angle, θ is the pitch angle, q is the pitch angular velocity and, let $(F_T, \delta_e) \in \mathbb{R}^2$ be the control input vector where F_T is the engine thrust and δ_e the elevator angle. Thus, the equations of motion of the aircraft longitudinal flight dynamics from [10] are

$$\dot{V}_a = \frac{1}{m}\left(-D + F_T \cos\alpha - mg\sin\gamma\right), \quad (1)$$

$$\dot{\gamma} = \frac{1}{mV_a}\left(L + F_T \sin\alpha - mg\cos\gamma\right), \quad (2)$$

$$\dot{\theta} = q, \quad (3)$$

$$\dot{q} = \frac{M(\delta_e)}{I_y}, \quad (4)$$

where we have introduced some abuse of notation for compactness since the angle of attack $\alpha(\theta, \gamma) = \theta - \gamma$ is not considered as an additional state; m and I_y are the mass and the inertia; and L, D and $M(\delta_e)$ are the aerodynamics forces lift, drag and pitching moment, respectively. In Fig. 1 a detailed definition of the forces, moments, and velocities are shown.
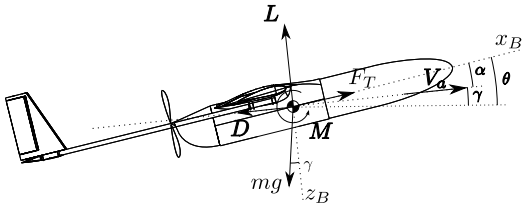

Fig. 1.   Definition of forces, moments and angles.

The aerodynamic forces and moments are computed through their non-dimensional coefficients as follows

$$L = \frac{1}{2}\rho V_a^2 S C_L, \; D = \frac{1}{2}\rho V_a^2 S C_D, \; M = \frac{1}{2}\rho V_a^2 S\bar{c}C_m(\delta_e), \quad (5)$$

where ρ is the air density, S is the reference wing surface, $\bar{c}$ is the mean chord and C_L, C_D and $C_m(\delta_e)$ are the lift, drag and pitching moment coefficients, respectively. Moreover, we consider the following models for the drag and moment coefficients (see for instance [11], [12] and [13]):

$$C_D = C_{D_0} + k_1 C_L + k_2 C_L^2, \quad (6)$$

$$C_m(\delta_e) = C_{m_0} + C_{m_\alpha}\alpha + C_{m_q}q + C_{m_{\delta_e}}\delta_e, \quad (7)$$

where C_{D_0}, k_1, k_2, C_{m_0}, C_{m_α}, C_{m_q} and $C_{m_{\delta_e}}$ are aircraft aerodynamic coefficients. In this work, all coefficients are considered to be unknown parameters, except for the well-known fact that $C_{m_{\delta_e}} < 0$. This is an improvement over [9] where knowledge of $C_{m_{\delta_e}}$ was assumed in the design.

Regarding the lift coefficient model, only the following assumption is considered.

Assumption 1: The lift coefficient C_L is only a function of α. The reference axis x_B is chosen so that $C_L(0) = 0$, i.e. x_B is parallel to the aircraft zero-lift line. Then, the property $x \cdot C_L(x) \geq 0$ is satisfied for all $x \in \mathbb{R}$.

This assumption is satisfied by all conventional airplanes in the non-stalled regime[1]. We underscore that this is the only assumption about C_L, which otherwise is considered completely unknown.

III. CONTROLLER DESIGN

The control objective is to design feedback laws for (F_T, δ_e) which make the system seek for known references in velocity and flight path angle (V_r, γ_{ref}). In [9], as a first attempt to solve this control problem, we designed a full-state control law accomplishing this objective. However, while the state vector (V_a, γ, θ, q) is physically measurable in an aircraft, the reference value θ_{ref} needed to reach the flight condition (V_r, γ_{ref}) is unknown and so, the state error $\theta - \theta_{ref}$ used in [9] is not measurable. It is shown below that $\theta_{ref} = \alpha_0 + \gamma_{ref}$, with α_0 being the trim angle of attack, which is not known since it depends on the desired flight condition (V_r, γ_{ref}) and on the lift coefficient function C_L. Thus, our previously derived full-state control law has to be suitably modified to obtain an output feedack law not requiring the knowledge of θ_{ref}.

The controller is designed considering first the velocity dynamics, given by Equation (1), and then the pitch dynamics given by (2)–(4). Thus, two different controllers are designed: the aerodynamic velocity is controlled using only the thrust (F_T) and the flight path angle (pitch dynamics) is controlled with the elevator angle (δ_e). The compound controller makes the closed-loop system follows the references as desired. Even though the novelties with respect to [9] are only on the flight-path-angle control design (Section III-B), for the sake of completeness, we reproduce next in Section III-A the design of the velocity control law; we refer the reader to [9] for the proof of stability.

---

[1]See for instance [14], where an extensive compendium of lift curves with this property can be found.

A. Control of aerodynamic velocity

The velocity dynamics are governed by the equation (1), where after substituting the moment model D from (5) reads

$$\dot{V}_a = \frac{1}{m}\left(-\frac{1}{2}\rho V_a^2 S C_D + F_T \cos\alpha - mg\sin\gamma\right), \quad (8)$$

where α and γ are measurable quantities and the engine thrust F_T is the control input. In addition, based on (6), we use the following drag model:

$$C_D = C_{D_0} + k_1\alpha + k_2\alpha^2, \quad (9)$$

where C_{D_0}, k_1 and k_2 are unknown parameters. Denote V_r to the reference velocity and define the error $z_V := V_a - V_r$. Thus, the evolution of the error from (8) becomes

$$
\begin{aligned}
\dot{z}_V &= -\frac{1}{2m}\rho(z_V + V_r)^2 S\varphi_V(\alpha)^T \cdot \boldsymbol{\theta}_V + F_T\frac{\cos\alpha}{m} \\
&\quad -g\sin\gamma - \dot{V}_r \\
&= -\beta_1\left(z_V^2 + V_r^2 + 2z_V V_r\right)\varphi_V(\alpha)^T \cdot \boldsymbol{\theta}_V \\
&\quad + F_T\frac{\cos\alpha}{m} - g\sin\gamma - \dot{V}_r,
\end{aligned}
\quad (10)
$$

where we have defined

$$\varphi_V(\alpha) := \begin{bmatrix}1 & \alpha & \alpha^2\end{bmatrix}^T, \boldsymbol{\theta}_V := [C_{D_0}\ k_1\ k_2]^T, \beta_1 := \frac{\rho S}{2m}, \quad (11)$$

where $\boldsymbol{\theta}_V \in \mathbb{R}^3$ is the unknown parameters vector, the $\varphi_V \in \mathbb{R}^3$ is defined using (9) as $C_D = \varphi_V(\alpha)^T \cdot \boldsymbol{\theta}_V > 0$ and it holds that $\beta_1 > 0$.

The velocity controller is formally stated in the following Proposition.

Proposition 1: Consider the system (10) and let $\hat{\boldsymbol{\theta}}_V$ be the estimate of $\boldsymbol{\theta}_V$ defined in (11). The *adaptative-state feedback* law given by

$$
\begin{aligned}
F_T &= \frac{m}{\cos\alpha}\left(g\sin\gamma + \dot{V}_r + \beta_1(z_V^2 + V_r^2)\varphi_V(\alpha)^T \cdot \hat{\boldsymbol{\theta}}_V\right. \\
&\quad \left. -\kappa_{V_1} z_V\right),
\end{aligned}
\quad (12)
$$

$$\dot{\hat{\boldsymbol{\theta}}}_V = -\beta_1\left(z_V^3 + z_V V_r^2\right)\boldsymbol{\Gamma}_V\varphi_V(\alpha), \quad (13)$$

guarantees global boundedness of z_V and $\hat{\boldsymbol{\theta}}_V$ and convergence of z_V to zero.

Proof: The proof is given in [9]. ∎

B. Control of the flight path angle

In this section a new adaptive output-feedback controller for the flight path angle is proposed, improving the adaptive full-state design given in [9]. There are two novelties with respect to [9]. On the one hand, the value α_0 is considered unknown, which leads to a more involved output-feedback design. On the other hand, the parameter $C_{m_{\delta_e}}$ is here considered unknown but negative. Both α_0 and $C_{m_{\delta_e}}$ were considered known in [9], paving the way for the design provided here; these improvements are far from being just trivial extensions.

The pitch dynamics are governed by equations (2)–(4) after substituting (5) and (12). We next state some assumptions regarding the pitch dynamics.

Assumption 2: The following assumptions are made:
- It is assumed that $\cos\gamma \approx \cos\gamma_{ref}$, as proposed in [5].
- $\dot{\gamma}_{ref}$ is assumed to be zero.
- Aircraft engines can not produce negative thrust. Thus F_T is always nonnegative.

Under Assumption 2 the equation (2) becomes

$$\dot{\gamma} = f(\alpha) = f(\theta - \gamma), \quad (14)$$

where the scalar function f is defined as

$$f(\alpha) := \frac{1}{mV_a}\left(\frac{1}{2}\rho V_a^2 S C_L(\alpha) + F_T\sin\alpha - mg\cos\gamma_{ref}\right).$$

Note that f depends implicitly on γ_{ref}.

Property 1: Let α_0 be the trim angle of attack, which is the value of α that makes $f(\alpha)$ zero (for a given γ_{ref}), i.e., $f(\alpha_0) = 0$. Then, under the Assumption 1, the function $f(\alpha)$ satisfies $(\alpha - \alpha_0)f(\alpha) > 0$. Since $f(\alpha)$ is unknown, α_0 is not computable. In addition, in what follows α_0 is assumed to be constant.

Let us first shift the equilibrium to zero defining the following vector of error coordinates $z \in \mathbb{R}^3$ as

$$z = \begin{bmatrix} z_1 \\ z_2 \\ z_3 \end{bmatrix} := \begin{bmatrix} \gamma - \gamma_{ref} \\ \theta - \gamma_{ref} - \alpha_0 \\ q \end{bmatrix} \quad (15)$$

Note that since α_0 is unknown it follows that z_2 is not a measurable quantity by itself. The equations (2)–(4) together with (14) in the new set of coordinates read

$$\dot{z}_1 = \eta(z_2 - z_1), \quad (16)$$

$$\dot{z}_2 = z_3, \quad (17)$$

$$
\begin{aligned}
\dot{z}_3 = &\ \beta_2\left[C_{m_0} + C_{m_\alpha}(z_2 - z_1 + \alpha_0)\right. \\
&\left. + C_{m_q}z_3 + C_{m_{\delta_e}}\delta_e\right],
\end{aligned}
\quad (18)
$$

where we have defined $\beta_2 := \frac{\rho V_a^2 S\bar{c}}{2I_y}$ and

$$\eta(x) := f(x + \alpha_0). \quad (19)$$

Notice that Property 1 makes the scalar function $\eta(x)$ to satisfy $x \cdot \eta(x) \geq 0$.

The control problem. To make the origin of (16)–(18) asymptotically stable, that with (15) becomes $(\gamma, \theta, q) = (\gamma_{ref}, \theta_{ref}, 0)$, through the input δ_e and under the following conditions:

C1. γ_{ref} is a given reference.
C2. α_0 is unknown and so, $\theta_{ref} := \alpha_0 + \gamma_{ref}$ too.
C3. $C_{m_{\delta_e}}$ from (7) is unknown but assumed to be negative.
C4. The measurable output vector $y \in \mathbb{R}^3$ is defined as

$$y := \begin{bmatrix} \gamma - \gamma_{ref} \\ \alpha \\ q \end{bmatrix} \equiv \begin{bmatrix} z_1 \\ z_2 - z_1 + \alpha_0 \\ z_3 \end{bmatrix}. \quad (20)$$

Remark 1: This control objective differs from [9] in the conditions C2, C3 and C4, making the design more involved. By dropping the assumption of knowledge of α_0 and $C_{m_{\delta_e}}$, the control law designed in [9] is no longer implementable.

Remark 2: A backstepping control law was designed in [5] for the cascade structure (16)–(18), but using in (4) the

aerodynamic moment model M as the control input. Then, a control allocation scheme was used to estimate the elevator deflections δ_e; additionally, Property 1 was invoked assuming knowledge of α_0. In this work $M(\delta_e)$ is a function of the physical control input δ_e, given by (7) with all aerodynamic coefficients unknown.

In what follows, we stabilize each step of the cascade explicitly using the backstepping approach.

Step 1. First, equation (16) is stabilized using z_2 as a virtual control. Defining the Lyapunov function as

$$W_1 = \frac{1}{2}z_1^2,$$

the derivative reads $\dot{W}_1 = z_1\eta(z_2 - z_1)$; we select the control $z_2 = u_1(z_1) = -\kappa_{\gamma_1}z_1$, where notice that $z_1 = y_1$ and thus measurable. Thus,

$$\dot{W}_1|_{z_2=u_1(z_1)} = z_1\eta(-(1 + \kappa_{\gamma_1})z_1),$$

and hence $\dot{W}_1|_{z_2=u_1(z_1)}$ is negative definite for $\kappa_{\gamma_1} > -1$.

Step 2. Defining now the error variable

$$\tilde{z}_2 := z_2 - u_1(z_1),$$

the equations (16)–(17) can be rewritten as

$$\dot{z}_1 = \eta(\tilde{z}_2 - (1 + \kappa_{\gamma_1})z_1), \tag{21}$$
$$\dot{\tilde{z}}_2 = z_3 + \kappa_{\gamma_1}\eta(\tilde{z}_2 - (1 + \kappa_{\gamma_1})z_1), \tag{22}$$

The Lyapunov function for (21)–(22) is

$$W_2 = c_1 W_1 + \int_0^{\tilde{z}_2-(1+\kappa_{\gamma_1})z_1} \eta(s)\,ds,$$

which is a positive definite function by the Property 1. Calculating $\dot{W}_2$ we get

$$\dot{W}_2 = c_1 z_1\eta + (-\eta + z_3)\eta$$
$$= -\eta^2 + (c_1 z_1 + z_3)\eta, \tag{23}$$

where we have omitted the argument of η for clarity, minding that $\eta = \eta(\tilde{z}_2 - (1 + \kappa_{\gamma_1})z_1)$. Selecting the virtual control as $z_3 = u_2(z_1) = -c_1 z_1$, (23) becomes $\dot{W}_2 = -\eta^2$ and then negative semidefinite, using again only the available output y_1. Invoking LaSalle's theorem, z_1 and $\tilde{z}_2$ tend to the largest invariant set inside the set $\{(z_1, \tilde{z}_2) \in \mathbb{R}^2 : \eta = 0\}$ which in turn implies from Property 1 and (19) that $\tilde{z}_2 - (1 + \kappa_{\gamma_1})z_1 = 0$. The residual dynamics on this set become

$$\dot{z}_1 = 0, \tag{24}$$
$$\dot{\tilde{z}}_2 = -c_1 z_1, \tag{25}$$

and then (24) implies that z_1 a constant. The derivative of the set is $\dot{\tilde{z}}_2 - (1 + \kappa_{\gamma_1})\dot{z}_1 = 0$, so it follows that $\dot{\tilde{z}}_2 = 0$, which together with (25) implies that the largest invariant set is the origin $z_1 = \tilde{z}_2 = 0$. Moreover, since W_2 is radially unbounded the origin is globally asymptotically stable. Notice that this implies $\gamma \to \gamma_{ref}$, $\theta \to \theta_{ref}$ even though θ_{ref} is unknown, or equivalently $\alpha \to \alpha_0$ with α_0 unknown.

Remark 3: In [9] an additional term was added to the Lyapunov function in this step, to get a negative term in $\tilde{z}_2^2$ in

the derivative, allowing to conclude exponential convergence but with the exact knowledge of α_0 needed in the resulting control law. Here, the use of $\tilde{z}_2$ in the virtual control law has been avoided by omitting that $\tilde{z}_2^2$ term, which in turn allows to avoid the knowledge of α_0. This improvement comes at the cost of not obtaining exponential stability, which implies some loss of robustness with respect to unmodeled dynamics.

Remark 4: This virtual control law does not need the function $f(\alpha)$, since the integral in the Lyapunov function W_2 (first introduced in [15]) has been used to avoid cancellations of the terms associated to η, which would introduce extra terms in the controller.

Step 3. In this last step, we extend the backstepping design to generate the elevator deflections laws. We employ an adaptive scheme to estimate online the aerodynamic moment coefficients. As commented before a further improvement upon [9] comes from dropping the hypothesis that $C_{m_{\delta_e}}$ is known. Only the physical fact that $C_{m_{\delta_e}} < 0$ is used.

The system, for this last step of the design, is composed by the subsystem (21)-(22) and the equation (18) in the new error coordinate defined as $\tilde{z}_3 := z_3 - u_2(z_1)$, and then becomes

$$\dot{z}_1 = \eta, \tag{26}$$
$$\dot{\tilde{z}}_2 = \tilde{z}_3 - c_1 z_1 + \kappa_{\gamma_1}\eta, \tag{27}$$
$$\dot{\tilde{z}}_3 = \beta_2 C_{m_{\delta_e}}\left(\boldsymbol{\varphi}_\gamma^T \cdot \boldsymbol{\theta}_\gamma + \delta_e\right) - \beta_2 \kappa_{\gamma_3}\tilde{z}_3 + c_1\eta, \tag{28}$$

where we have defined a scaled vector from (7) of unknown aerodynamic coefficients $\boldsymbol{\theta}_\gamma \in \mathbb{R}^4$ as

$$\boldsymbol{\theta}_\gamma := \begin{bmatrix} \dfrac{C_{m_0}}{C_{m_{\delta_e}}} & \dfrac{C_{m_\alpha}}{C_{m_{\delta_e}}} & \dfrac{C_{m_q}}{C_{m_{\delta_e}}} & \dfrac{1}{C_{m_{\delta_e}}} \end{bmatrix}^T, \tag{29}$$

and a vector of measurable quantities $\boldsymbol{\varphi}_\gamma(y) \in \mathbb{R}^4$ as

$$\boldsymbol{\varphi}_\gamma(y) := \begin{bmatrix} 1 \\ \alpha \\ z_3 \\ \kappa_{\gamma_3}\tilde{z}_3 \end{bmatrix} = \begin{bmatrix} 1 \\ y_2 \\ y_3 \\ \kappa_{\gamma_3}(y_3 + c_1 y_1) \end{bmatrix}, \tag{30}$$

and recall that δ_e is the elevator deflection, which is the real control input of the aircraft.

Remark 5: The controller proposed in this step is designed to stabilize the system (26)–(28) with an adaptation law to estimate the parameters (29) and using the only available outputs given by (20).

Let us define the compound Lyapunov function as

$$W_3 = W_2 + \frac{c_3}{2}\tilde{z}_3^2 + \frac{|C_{m_{\delta_e}}|}{2}\tilde{\boldsymbol{\theta}}_\gamma^T \boldsymbol{\Gamma}_\gamma^{-1}\tilde{\boldsymbol{\theta}}_\gamma, \tag{31}$$

where $c_3 > 0$, $\boldsymbol{\Gamma}_\gamma = \boldsymbol{\Gamma}_\gamma^T > 0$ is the adaptation gain matrix, $\hat{\boldsymbol{\theta}}_\gamma$ is the estimate of $\boldsymbol{\theta}_\gamma$ and $\tilde{\boldsymbol{\theta}}_\gamma := \boldsymbol{\theta}_\gamma - \hat{\boldsymbol{\theta}}_\gamma$ is the estimation error vector.

The Lyapunov function derivative becomes

$$\dot{W}_3 = -\eta^2 + \tilde{z}_3\eta + c_3\tilde{z}_3\beta_2 C_{m_{\delta_e}}\left(\boldsymbol{\varphi}_\gamma^T \cdot \boldsymbol{\theta}_\gamma + \delta_e\right)$$
$$+ c_3\tilde{z}_3 c_1\eta - c_3\beta_2\kappa_{\gamma_3}\tilde{z}_3^2 + |C_{m_{\delta_e}}|\tilde{\boldsymbol{\theta}}_\gamma^T \boldsymbol{\Gamma}_\gamma^{-1}\dot{\hat{\boldsymbol{\theta}}}_\gamma. \tag{32}$$

Defining the control and the adaptation laws as

$$\delta_e := -\boldsymbol{\varphi}_\gamma^T \cdot \hat{\boldsymbol{\theta}}_\gamma, \tag{33}$$

$$\dot{\hat{\boldsymbol{\theta}}}_\gamma = -\dot{\tilde{\boldsymbol{\theta}}}_\gamma := -c_3 \beta_2 \tilde{z}_3 \boldsymbol{\Gamma}_\gamma \boldsymbol{\varphi}_\gamma, \tag{34}$$

and selecting $c_3 = \frac{1}{c_1}$ then (32) yields

$$
\begin{aligned}
\dot{W}_3 &= -\eta^2 + 2\tilde{z}_3\eta - \frac{\beta_2 \kappa_{\gamma_3}}{c_1}\tilde{z}_3^2 \\
&\leq -\left(1 - \frac{2}{\lambda}\right)\eta^2 - \left(\frac{\beta_2 \kappa_{\gamma_3}}{c_1} - 2\lambda\right)\tilde{z}_3^2,
\end{aligned}
$$

where we used the Young's inequality with the parameter λ still free. Thus, pick $\lambda = 4$ and $\kappa_{\gamma_3} > 8c_1/\beta_2$ and we get

$$\dot{W}_3 \leq -\frac{1}{2}\eta^2 - \frac{1}{2}\tilde{z}_3^2,$$

which is a negative semidefinite function, as before. Invoking again LaSalle's theorem, it is straightforward to see that the largest invariant set inside the set $\{(z_1, \tilde{z}_2, \tilde{z}_3) \in \mathbb{R}^3 : \eta = 0, \tilde{z}_3 = 0\}$ is the origin $z_1 = \tilde{z}_2 = \tilde{z}_3 = 0$, because $z_1 = \tilde{z}_2 = 0$ implies $z_2 = 0$ by the same arguments as before, and additionally $z_1 = 0$ and $\tilde{z}_3 = 0$ implies directly $z_3 = 0$. We formally summarize the result obtained in this section in the following Proposition and in the original coordinates.

Proposition 2: Consider the flight-path-angle dynamics (2)–(4) under Assumptions 1 and 2, with the only measurable outputs given by (20) and being $\hat{\boldsymbol{\theta}}_\gamma$ the estimate of $\boldsymbol{\theta}_\gamma$ defined in (29). Then, the *adaptive output-feedback* given by

$$\delta_e = -\boldsymbol{\varphi}_\gamma(y)^T \cdot \hat{\boldsymbol{\theta}}_\gamma, \tag{35}$$

$$\dot{\hat{\boldsymbol{\theta}}}_\gamma = -\frac{\beta_2}{c_1}\left(q + c_1(\gamma - \gamma_{ref})\right)\boldsymbol{\Gamma}_\gamma \boldsymbol{\varphi}_\gamma(y), \tag{36}$$

with $c_1 > 0$ and $\kappa_{\gamma_3} > 8c_1/\beta_2$, $\boldsymbol{\Gamma}_\gamma = \boldsymbol{\Gamma}_\gamma^T > 0$ and

$$\boldsymbol{\varphi}_\gamma(y) = \begin{bmatrix} 1 \\ \alpha \\ q \\ \kappa_{\gamma_3}(q + c_1(\gamma - \gamma_{ref})) \end{bmatrix}, \tag{37}$$

assures that the equilibrium manifold $(\gamma, \theta, q, \hat{\boldsymbol{\theta}}_\gamma) = (\gamma_{ref}, \theta_{ref}, 0, \hat{\boldsymbol{\theta}}_\gamma^*)$ is globally asymptotically stable, for some constant $\hat{\boldsymbol{\theta}}_\gamma^*$.

Proof: The proposed Lyapunov function (31) is positive definite and radially unbounded which, together with the *adaptive output-feedback* (33)–(34), or equivalently (35)–(36), makes $\dot{W}_3 \leq 0$ and then, by LaSalle-Yoshizawa theorem we conclude global boundedness $(z_1, \tilde{z}_2, \tilde{z}_3)$, or equivalently $(\gamma, \theta, q, \hat{\boldsymbol{\theta}}_\gamma)$. Since the whole closed-loop system is time-invariant we can invoke LaSalle's invariance principle assuring that all trajectories converge to the largest invariant set contained in $\{(z_1, \tilde{z}_2, \tilde{z}_3, \hat{\boldsymbol{\theta}}_\gamma) \in \mathbb{R}^4 : \dot{W}_3 = 0\}$. Since it is a cascade system the backwards analysis of the residual dynamics done along the design steps holds, where we concluded $(z_1, \tilde{z}_2, \tilde{z}_3) = (0,0,0)$. Thus, since all trajectories are bounded then we conclude that the equilibrium manifold $(\tilde{z}_3, \tilde{z}_2, z_1, \hat{\boldsymbol{\theta}}_\gamma) = (0, 0, 0, \hat{\boldsymbol{\theta}}_\gamma^*)$, or equivalently $(\gamma, \theta, q, \hat{\boldsymbol{\theta}}_\gamma) = (\gamma_{ref}, \theta_{ref}, 0, \hat{\boldsymbol{\theta}}_\gamma^*)$, is globally asymptotically stable. ∎

Remark 6: A comment about the stability of the whole aircraft longitudinal closed-loop dynamics is in order. Notice that the controllers were designed separately, and moreover, in the construction of the flight path angle controller the assumption of F_T being non-negative was made. Although this assumption is enough to keep the aerodynamic properties unchanged (in particular, Property 1), the control law for the aerodynamic velocity does not enforce this physical constraint, i.e., there are no guarantees that F_T avoids the zero crossing. This is currently under investigation since, in the light of the simulation results (see next Section), it looks that under some mild extra assumptions the global boundedness and convergence are guaranteed.

IV. SIMULATION RESULTS

In this section, simulation results of the controllers developed are shown. The simulation model is composed of Equations (1)–(4), and the aerodynamic model of Cefiro UAV, developed by the University of Seville [8].

For a more realistic simulation, saturations in the control signals are also considered. Thus, the following limits are introduced in the thrust and elevator angle:

$$F_T \in [4.9\,\text{N}, \ 117.6\,\text{N}], \ \delta_e \in [-30^\circ, \ 30^\circ]. \tag{38}$$

The tuning parameters for the velocity controller are

$$\kappa_{V_1} = 10; \quad \boldsymbol{\Gamma_V} = 0.001\boldsymbol{I}_3,$$

where $\boldsymbol{I}_3$ is the identity matrix of dimension 3. For the flight path angle controller, the parameters are

$$\kappa_{\gamma_3} = 3; \quad c_1 = 1; \quad \boldsymbol{\Gamma_\gamma} = 0.5 \begin{bmatrix} 1 & 0 & 0 & 0 \\ 0 & 1 & 0 & 0 \\ 0 & 0 & 1 & 0 \\ 0 & 0 & 0 & 20 \end{bmatrix}.$$

The initial estimate of the unknown parameters is

$$
\begin{aligned}
\hat{\boldsymbol{\theta}}_V &= \begin{bmatrix} 0.05 & 0.05 & 0.05 \end{bmatrix}^T, \\
\hat{\boldsymbol{\theta}}_\gamma &= \begin{bmatrix} 0.5 & 1 & 15 & -0.3 \end{bmatrix}^T.
\end{aligned}
$$

The reference maneuver selected is as follows. The velocity profile consist on three segments with constant velocity, separated by uniform acceleration and uniform deceleration segments. The flight path angle profile consist on six different segments with constant values of the flight path angle.

Fig. 2 shows the time evolution of the aerodynamic velocity. After an initial period with some oscillations in which saturations in thrust occurs, the velocity controller achieves an excellent agreement with the reference even when a constant acceleration is demanded. Fig. 4 shows the control signals. In the figure, the dashed line represent the *computed* control signal, whereas the solid line represents the *commanded* control signal (with saturations). Notice that although thrust saturation is present at the beginning of the simulation (since the engine is not allowed to produce negative thrust) the reference value is successfully reached.

Regarding the flight path angle controller, in Fig. 3 it can be seen that convergence to the reference is also achieved,

but with at a slower rate since smaller gains were selected. The reference flight path angle values are reached without excessive oscillation and there are no permanent regime errors, even without the knowledge of any value of any aerodynamic coefficient. Fig. 4 shows the computed (dashed) and commanded (solid) elevator input. It can be seen that, when instantaneous changes in flight path angle are demanded, the controller tends to apply high elevator deflections, beyond the maximum values. However, even in the presence on saturation, the stability of the system is not compromised and convergence to the reference values is maintained.

Fig. 5 shows other state variables such as pitch, attack angle, and pitch angular velocity, which are kept within reasonable values during the maneuver. Finally, Fig. 6 shows the time evolution of the estimated parameters, which converge towards certain constant values.
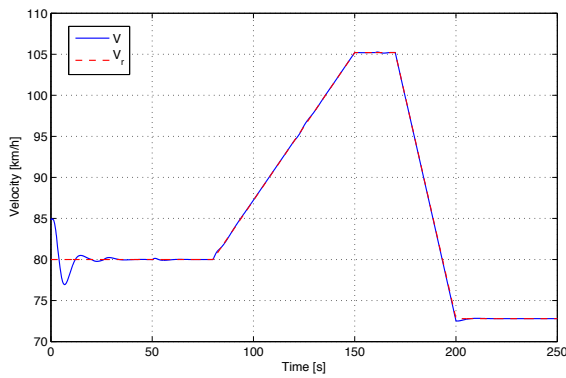

Fig. 2. Time evolution of the aerodynamic velocity (solid), compared with its reference (dashed).
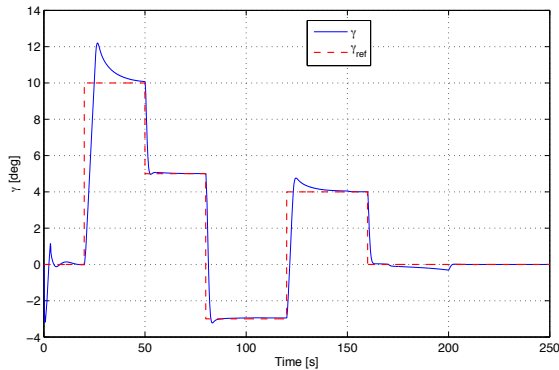

Fig. 3. Time evolution of the flight path angle (solid) compared with its reference (dashed).

V. CONCLUSION

In this work, we presented the design of an adaptive and output-feedback controller for the longitudinal flight dynamics of an UAV that is able to make the aircraft follow references in velocity and flight path angle. The design is build upon our previously developed full-state control law [9], it is explicit, easy to implement, only employs
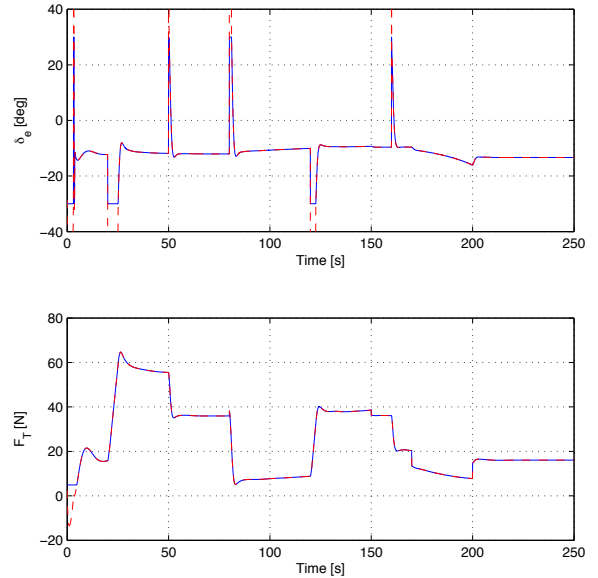

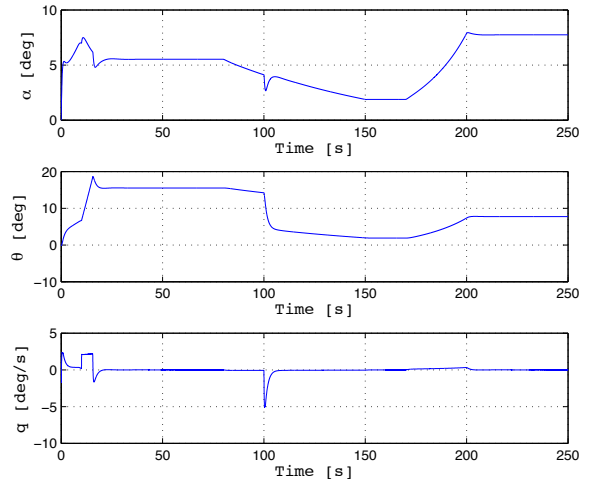Fig. 4. Control signals: computed (dashed) and commanded (solid), which includes saturation.

Fig. 5. Time evolution of the angles of attack α and pitch θ, and the angular velocity q.

measurable quantities, and does not require any knowledge of the aerodynamics model. Simulations show that the controller can make the system follow the references, even in the presence of actuator saturations. The simulations were performed using a realistic UAV model, the Cefiro aircraft developed by the University of Seville. As a next step, we will work on dropping some of the assumptions made in the paper. Also, the control laws will be implemented on board the aircraft to perform experiments and further validate the results.

REFERENCES

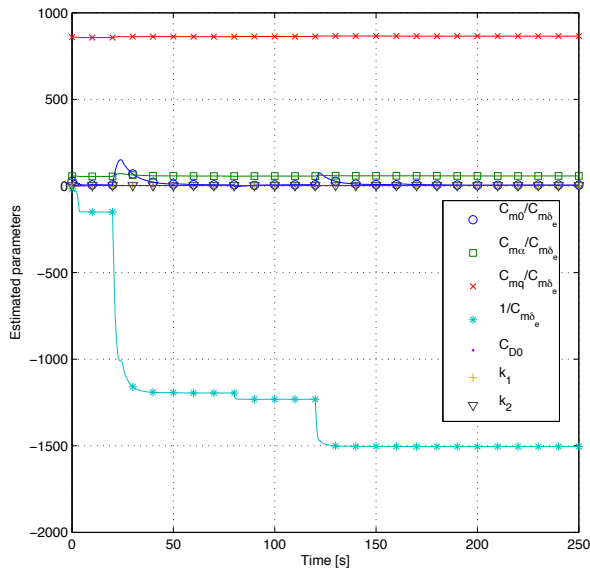[1] Donald McLean, *Automatic Flight Control Systems*, Prentice Hall, 1990.

Fig. 6. Time evolution of the estimated parameters and aerodynamic coefficients, showing convergence to some values.

[2] Robert A. Nichols, Robert T. Reichert, and Wilson J. Rugh, "Gain scheduling for H_∞ controllers: A flight control example," *IEEE Trans. Contr. Syst. Tech.*, vol. 1, no. 2, pp. 69–78, 1993.

[3] Yoshimasa Ochi and Kimio Kanai, "Design of restructurable flight control systems using feedback linearization," *J. Guid. Contr. Dynam.*, vol. 14, no. 5, pp. 903–911, 1991.

[4] Miroslav Krstić, Ioannis Kanellakopoulos, and Petar Kokotović, *Nonlinear and Adaptive Control Design*, John Wiley, 1995.

[5] Ola Härkegård, *Backstepping and Control Allocation with Applications to Flight Control*, Ph.D. thesis, Linköping Universtity, 2003.

[6] J. Farrell, M. Sharma, and M. Polycarpou, "Backstepping-based flight control with adaptive function approximation," *J. Guid. Contr. Dynam.*, vol. 28, no. 6, pp. 1089–1102, 2005.

[7] L. Sonneveldt, Q.P. Chu, and J.A. Mulder, "Nonlinear flight control design using constrained adaptive backstepping," *J. Guid. Contr. Dynam.*, vol. 30, no. 2, pp. 322–336, 2007.

[8] Carlos Bernal, Andrés Fernandez, Pedro Lopez, Adrian Martin, Daniel Perez, Francisco Samblas, Sergio Esteban, Francisco Gavilan, and Damian Rivas, "Cefiro: an aircraft design project in the university of seville," in *9th European Workshop on Aircraft Design Education (EWADE 2009)*, 2009.

[9] Francisco Gavilan, Jose Angel Acosta, and Rafael Vazquez, "Control of the longitudinal flight dynamics of an uav using adaptive backstepping," in *IFAC World Congress*, 2011.

[10] B. L. Stevens and F. L. Lewis, *Aircraft Control and Simulation*, John Wiley, Second edition, 2003.

[11] Bernard Etkin and Lloyd D. Reid, *Dynamics of Flight. Stability and Control*, John Wiley, 3rd edition, 1996.

[12] Bandu N. Pamadi, *Performance, Stability, Dynamics, and Control of Airplanes*, AIAA, 2nd edition, 2004.

[13] Louis V. Schmidt, *Introduction to Aircraft Flight Dynamics*, AIAA, 1998.

[14] Ira H. Abot and Albert E. Von Doenhoff, *Theory of wings and sections*, Dover, 1959.

[15] Miroslav Krstic and Petar V. Kokotovic, "Lean backstepping design for a jet engine compressor model," in *IEEE Conference on Control Applications*, 1995, pp. 1047–1052.